

Effects of temperature and pressure on OH laser-induced fluorescence exciting A-X (1,0) transition at high pressures

Xiaobo Tu(涂晓波), Linsen Wang(王林森), Xinhua Qi(齐新华), Bo Yan(闫博), Jinhe Mu(母金河), Shuang Chen(陈爽)

Citation: Chin. Phys. B . 2020, 29(9): 093301 . **doi:** 10.1088/1674-1056/aba5ff
Journal homepage: http://cpb.iphy.ac.cn; http://iopscience.iop.org/cpb

What follows is a list of articles you may be interested in

Energy transfer, luminescence properties, and thermal stability of color tunable barium pyrophosphate phosphors

Meng-Jiao Xu(徐梦姣), Su-Xia Li(李素霞), Chen-Chen Ji(季辰辰), Wan-Xia Luo(雒晚霞), Lu-Xiang Wang(王鲁香)
Chin. Phys. B . 2020, 29(6): 063301 . **doi:** 10.1088/1674-1056/ab821a

Spectral attenuation of a 400-nm laser pulse propagating through a plasma filament induced by an intense femtosecond laser pulse

Quan-Jun Wang(王全军), Rao Chen(陈娆), Jia-Chen Zhao(赵家琛), Chun-Lin Sun(孙春霖), Xiao-Zhen Wang(王小珍), Jing-Jie Ding(丁晶洁), Zuo-Ye Liu(刘作业), Bi-Tao Hu(胡碧涛)
Chin. Phys. B . 2020, 29(1): 013301 . **doi:** 10.1088/1674-1056/ab5a39

Experimental optimum design and luminescence properties of $NaY(Gd)(MoO_4)_2$: Er^{3+} phosphors

Jia-Shi Sun(孙佳石), Sai Xu(徐赛), Shu-Wei Li(李树伟), Lin-Lin Shi(石琳琳), Zi-Hui Zhai(翟梓会), Bao-Jiu Chen(陈宝玖)
Chin. Phys. B . 2016, 25(6): 063301 . **doi:** 10.1088/1674-1056/25/6/063301

Exploring photocurrent output from donor/acceptor bulk-heterojunctions by monitoring exciton quenching

Wang Xin-Ping, He Zhi-Qun, Liang Chun-Jun, Qiu Hai-An, Jing Xi-Ping
Chin. Phys. B . 2015, 24(6): 063301 . **doi:** 10.1088/1674-1056/24/6/063301

High-pressure-activated carbon tetrachloride decomposition

Chen Yuan-Zheng, Zhou Mi, Sun Mei-Jiao, Li Zuo-Wei, Sun Cheng-Lin
Chin. Phys. B . 2014, 23(2): 023302 . **doi:** 10.1088/1674-1056/23/2/023302

Effects of temperature and pressure on OH laser-induced fluorescence exciting A–X (1,0) transition at high pressures*

Xiaobo Tu(涂晓波)[1,2], Linsen Wang(王林森)[2], Xinhua Qi(齐新华)[2], Bo Yan(闫博)[2], Jinhe Mu(母金河)[2], and Shuang Chen(陈爽)[2,†]

[1] *Science and Technology on Scramjet Laboratory, Hypervelocity Aerodynamics Institute, China Aerodynamics Research and Development Center, Mianyang* 621000, *China*
[2] *China Aerodynamics Research and Development Center, Mianyang* 621000, *China*

(Received 23 April 2020; revised manuscript received 11 July 2020; accepted manuscript online 15 July 2020)

The effects of temperature and pressure on laser-induced fluorescence (LIF) of OH are numerically studied under the excitation of A–X (1,0) transition at high pressures. A detailed theoretical analysis is carried out to reveal the physical processes of LIF. It is shown that high pressure LIF measurements get greatly complicated by the variations of pressure- and temperature-dependent parameters, such as Boltzmann fraction, absorption lineshape broadening, central-frequency shifting, and collisional quenching. Operations at high pressures require a careful choice of an excitation line, and the $Q_1(8)$ line in the A–X (1,0) band of OH is selected due to its minimum temperature dependence through the calculation of Boltzmann fraction. The absorption spectra of OH become much broader as pressure increases, leading to a smaller overlap integral and thus smaller excitation efficiency. The central-frequency shifting cannot be omitted at high pressures, and should be taken into account when setting the excitation frequency. The fluorescence yield is estimated based on the LASKIN calculation. Finally, OH-LIF measurements were conducted on flat stoichiometric CH_4/air flames at high pressures. And both the numerical and experimental results illustrate that the pressure dependence of fluorescence yield is dominated, and the fluorescence yield is approximately inversely proportional to pressure. These results illustrate the physical processes of OH-LIF and provide useful guidelines for high-pressure application of OH-LIF.

Keywords: laser-induced fluorescence, OH, high pressure, numerical analysis

PACS: 33.50.–j, 33.50.Dq, 47.70.Pq **DOI:** 10.1088/1674-1056/aba5ff

1. Introduction

Laser-induced fluorescence (LIF) is one of the most important and widely-used laser diagnostic techniques in combustion studies.[1–5] It has been utilized to measure temperature[1] and species concentration[2] and to visualize flame structures,[4,5] through the detection of intermediate species, such as OH, CH, and NO. Among them, OH benefits from its relatively high concentration in hydrocarbon combustion, strong absorption, and emission transitions in the ultraviolet, therefore it can be easily detected. More importantly, OH is a key intermediate in combustion kinetics,[6] making it an ideal and popular candidate in LIF measurement.

The most attractive merit of LIF is the possibility to perform two-dimensional (2D) measurements, leading to planar laser-induced fluorescence (PLIF). OH-PLIF has become a standard diagnostic tool in combustion studies, and has been playing an increasingly important role in diagnosing practical combustion devices, such as internal combustion engines and gas turbines. All of these devices operate at high pressures above 1 bar (1 bar = 10^5 Pa). Combustion diagnostics is therefore necessary to be carried out at high pressure to develop and validate combustion kinetic mechanisms.

However, it is not an easy task to interpret OH-PLIF in high-pressure combustion. The fluorescence is related to collisional energy transfer processes such as vibrational energy transfer (VET), rotational energy transfer (RET), and quenching. It is then a complex function of absolute OH concentration, pressure, temperature, and also the chemical composition of flame.[7] At high pressure, LIF measurements are even heavily influenced by collision-induced effects, such as absorption lineshape broadening, central-frequency shifting, and collisional quenching, which are all enhanced as pressure rises. These effects should be taken into account in the analysis of the fluorescence signal, whether it is relative or absolute concentration measurement. Thus it is necessary to quantify the influence of those effects according to pressure as well as other flame conditions. Unfortunately, only a few studies focus on this issue, and some related topics are scattered in several published papers.[7–9] Our previous study[9] aims at the analysis of the absolute measurement of OH, and pressure only covers 1 bar–10 bar.

In the present work, specific attention is paid to estimate the effects of temperature and pressure on OH-LIF at high

*Project supported by the National Natural Science Foundation of China (Grant Nos. 51976233 and 91641118).
†Corresponding author. E-mail: chenshuang827@gamil.com
© 2020 Chinese Physical Society and IOP Publishing Ltd

pressures via numerical analysis. A detailed theoretical analysis is carried out to reveal the physical processes of LIF. The temperature and pressure dependence of fluorescence is examined through three main parameters: Boltzmann fraction, overlap integral, and fluorescence yield. A suitable choice of the absorption line is done through calculation of Boltzmann fraction. High-pressure LIF measurements get complicated by the collision-induced effects, such as absorption lineshape broadening, central-frequency shifting, and collisional quenching. Absorption-line broadening and central-frequency shifting are calculated based on HITRAN database to evaluate the overlap integral. The fluorescence yield is estimated based on the LASKIN calculation, taking into consideration all energy transfer processes in the upper states of OH. Finally, OH-LIF measurements were conducted on flat stoichiometric CH_4/air flame at high pressures. The relationship between fluorescence and pressure was analyzed.

2. Theory

It is quite challenging to apply LIF to high-pressure combustion. One fundamental challenge comes from obtaining the fluorescence signal with an acceptable signal to noise ratio, since the fluorescence signal becomes much weaker at high pressures. A careful optimization of the excitation/detection scheme is needed, if one wanted to address the challenges of the high-pressure application of LIF. Many issues have to be considered, such as absorption line broadening and frequency shift, collisional transitions and quenching. It is of critical importance to understand the physical processes of LIF.

Laser-induced fluorescence originates from spontaneous emission of simulated atoms or molecules by laser radiation. In OH-LIF processes, the OH radicals are populated to an upper energy level by a laser beam with a wavelength tuning to a given transition line. The laser-populated OH radicals are not stable, some of which would directly return to the ground level through laser-induced stimulated emission. The population in the upper state would be re-distributed via rotational and vibrational energy transfer processes through collisions with other molecules. Also, collisions would make non-radiation transitions take place, which is referred to as collisional quenching. Spontaneous emissions take place when the OH radicals relax from the re-distributed upper states to the ground states, producing the fluorescence signal.

In the linear regime of OH-LIF, the detected fluorescence signal can be expressed as follows:[7]

$$I_{\mathrm{F}} = K n_{\mathrm{OH}} \left(\frac{E_\nu}{A}\right) \frac{f_{\mathrm{B}} B_{12}}{c^2} \int \phi_{\mathrm{laser}} \phi_{\mathrm{abs}} \,\mathrm{d}\nu \frac{A_{21}}{A_{21}+Q_{21}}, \quad (1)$$

where K is a constant that relates to the optical collection system and detector or camera, n_{OH} is the number density of OH, E_ν is the laser energy per pulse, A is the area of laser pulse beam, f_{B} is the Boltzmann factor of the ground level excited, B_{12} is the Einstein coefficient of stimulated absorption, $\int \phi_{\mathrm{laser}} \phi_{\mathrm{abs}} \mathrm{d}\nu$ is the overlap integral between the absorption line-shape ϕ_{abs} and laser profile ϕ_{laser}, $A_{21}/(A_{21}+Q_{21})$ is called the fluorescence yield in which A_{21} and Q_{21} correspond to the Einstein coefficient of spontaneous emission and collisional quenching respectively.

LIF signal is a function of OH properties (concentration and temperature), from Eq. (1), but also related to energy transfer processes, such as vibrational energy transfer, rotational energy transfer, and collisional quenching. These processes are state-dependent, and evaluation of these processes cannot be done without the knowledge of the upper state population as a function of time. Therefore the LASKIN code[10] is used to simulate the upper state population dynamic via solving the rate equations that govern the LIF process.

3. Simulation results and discussions

According to the previous theoretical analysis, the fluorescence signal in OH-LIF measurement depends on Boltzmann fraction, overlap integral, and fluorescence yield, which are all affected by pressure and temperature. The three factors will be numerically simulated and discussed in this section.

3.1. Excitation line selection

Usually, there are three exciting bands employed in OH-LIF applications: (0,0), (1,0), and (3,0) bands, because of the highest population in the ground $X^2\Pi$ ($v''=0$) state. Fluorescence of excitation within the (3,0) band is nearly free of quenching effect due to the rapid pre-dissociation of the OH $A^2\Sigma^+$ ($v'=3$) state. Unfortunately, the high pre-dissociative rate would cause the fluorescence quantum efficiency to decrease, making the fluorescence signal even weak and difficult to detect. The main drawback of excitation in the (0,0) band is that the fluorescence signals are in the same band, and it is impossible to distinguish the signal and the scattered laser light. A practical solution is to employ the non-resonant excitation/detection scheme. The technique allows the use of optical filters to suppress the scattered light. This is why it is very popular to detect the (0,0) and/or (1,1) band after exciting the (1,0) band in OH-LIF applications. Therefore excitation of (1,0) band is discussed in the present simulation.

The Boltzmann fractions are calculated and illustrated in Fig. 1 for the lowest ten rotational levels in the state $X^2\Pi$ ($v''=0$) of OH using the Eq. (8) of Ref. [11]. The total partition function is obtained using Dunham coefficients given in Ref. [12]. It is notable that the Boltzmann equation is only valid in thermal equilibrium. The OH radicals in flames can be regarded as equilibrated because the chemical reaction rate is much slower than the rate of energy transfer processes. The Boltzmann fraction depends only on the temperature for a

given level. As temperature increases, the OH radicals on the lower levels would jump to the higher levels. Consequently, the Boltzmann fraction declines on the low levels, while rises on the high levels. The Boltzmann fraction of level $J'' = 8.5$ presents the minimum temperature dependence over the common temperature domain of flames, 1500 K–2500 K. Considering that the Q_1 branch possesses the highest absorption coefficient, the $Q_1(8)$ line is perfect for OH-LIF and employed in the following discussions.

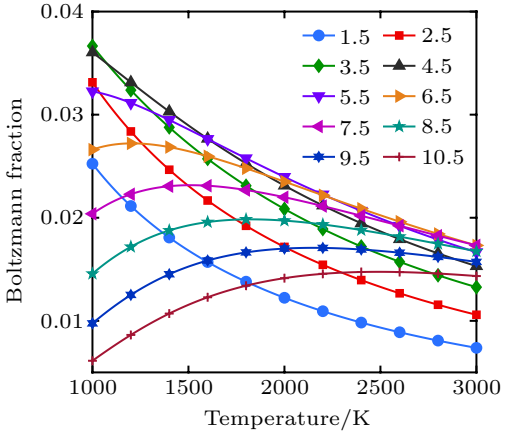


Fig. 1. Temperature dependence of Boltzmann fraction for different rotational levels in the state $X^2\Pi$ ($v'' = 0$) of OH.

3.2. Overlap integral

The overlap integral $\int \phi_{\text{laser}}\phi_{\text{abs}}\mathrm{d}\nu$ is an overall integral of spectrum overlap between the laser and absorption, revealing the excitation efficiency of the laser interacting with OH. It is common to assume that the lineshape of laser has a Lorentzian profile. The typical linewidth of a frequency-doubled dye laser is on the order of 0.1 cm^{-1}.[13] In this simulation, the laser linewidth is therefore assumed to be 0.1 cm^{-1}. The assumed laser profile is shown and denoted with solid cycles in Figs. 2(a) and 2(b). The laser wavelength is at 283.636 nm where the absorption line $Q_1(8)$ of A–X (1,0) band locates in vacuum.

The absorption lineshape of OH is usually described as Voigt profile that results from two broadening mechanisms, i.e., collisional broadening and Doppler broadening. The broadening parameter Γ_0 depends on temperature according to the power law, and can be expressed as follows:

$$\Gamma_0(p,T) = \gamma_0 T_{\text{ref}} \left(\frac{T_{\text{ref}}}{T}\right)^n p, \tag{2}$$

where T_{ref} is the reference temperature (usually at the room temperature 296 K), γ_0 is the broadening parameter at T_{ref}, n is exponent index describing the corresponding temperature dependence. The reference temperature T_{ref} and the corresponding broadening parameter γ_0 can be retrieved from the HITRAN database.[14] As to the exponent index n, the value of 0.66 is adopted according to Ref. [15].

Also, the absorption lineshift would take place as a consequence of collision when the pressure or temperature changes. However, the data for evaluating lineshift is lacking in the HITRAN database. The research of Davidson *et al.*[16] and Singla *et al.*[9] demonstrates that the collision-induced lineshift obeys linear dependence of pressure and exponent dependence of temperature:

$$\Delta\nu_S(p,T) = -0.0305 \left(\frac{p}{p_{\text{ref}}}\right)\left(\frac{T_{\text{ref}}}{T}\right)^{0.45}, \tag{3}$$

where the reference pressure and temperature are respectively $p_{\text{ref}} = 1$ bar and $T_{\text{ref}} = 296$ K.

The absorption spectra of the A–X (1, 0) $Q_1(8)$ line are calculated at temperatures varying from 1000 K to 3000 K and at high pressures varying from 1 bar to 30 bar. The calculation has counted in the effect of line-shift using a modified Python function base on the HAPI Python library.[17] Figures 2(a) and 2(b) show the cases of absorption spectra at different pressures and different temperatures, respectively. As the pressure rises, the absorption spectra become broad and red-shifted due to collision effects. But the situation is converse when the temperature increases. Increasing the temperature would narrow the absorption spectra, because the effect of Doppler broadening increases while that of collisional broadening decreases since the density decreases. Also the absorption spectra blue-shift when increasing temperature as a result of smaller lineshift due to the decreasing effect of collision broadening.

The calculated overlaps are shown in Figs. 2(c) and 2(d). The overlap decreases obviously when the pressure increases, which indicates that the collisional broadening dominates in the decrease of overlap. It is interesting that the overlap increases with the increase of temperature at low pressure, but decreases at high pressure. This is a consequence of competition between Doppler broadening and collisional broadening. The turning point of the trend is at a pressure of about 5 bar. Because the overlaps are very close at this pressure when temperature varying from 1000 K to 3000 K as it is demonstrated in Fig. 2(d) that all the lines cross near 5 bar.

In many practical applications of OH-LIF, such as gas turbines and engines, the pressure varies quickly with time and space, and is hardly determined. Therefore the excitation wavelength for OH-LIF is usually chosen according to the line position database of LIFBASE,[18] without considering the influence of lineshift, even at high pressure. The lineshift induced by collisions, however, would decrease the excitation efficiency. The overlaps and the corresponding overlap decreases are calculated for the tuning and detuning of laser frequency according to the line position of $Q_1(8)$ at 2000 K and 10 bar. For detuning case, the laser wavelength is tuned to 283.636 nm, the absorption line of $Q_1(8)$ in the vacuum.

The calculated results are shown in Fig. 3(a), where the laser linewidth varies from 0 to 1 cm^{-1}. (The laser lineshape for a zero linewidth is a Dirac δ function.) The overlap decrease falls when laser linewidth increases, however the overlap declines quickly. The overlap for a laser linewidth of 1 cm^{-1} is less than one third of that for 0.1-cm^{-1} linewidth. It is notable that, the detuning makes the overlap decrease about 13% for 0.1-cm^{-1} linewidth due to the lineshift, which would lead to an obvious decrease in excitation efficiency. A larger laser bandwidth is less sensitive to detuning, but would reduce the excitation efficiency. The overlap decreases are also calculated for different temperatures and pressures with a 0.1-cm^{-1} linewidth, as illustrated in Fig. 3(b). As the pressure rises, the overlap decrease grows quickly and reaches about 30% at 30 bar. Increasing temperature would slightly ease the growth of overlap decrease. Therefore, in order to maximize the excitation efficiency, it requires considerable attention to mitigate the effect of collision-induced lineshift, especially at high pressure. And the laser frequency should be tuning to the center of the absorption spectrum according to the predetermined or estimated pressure.

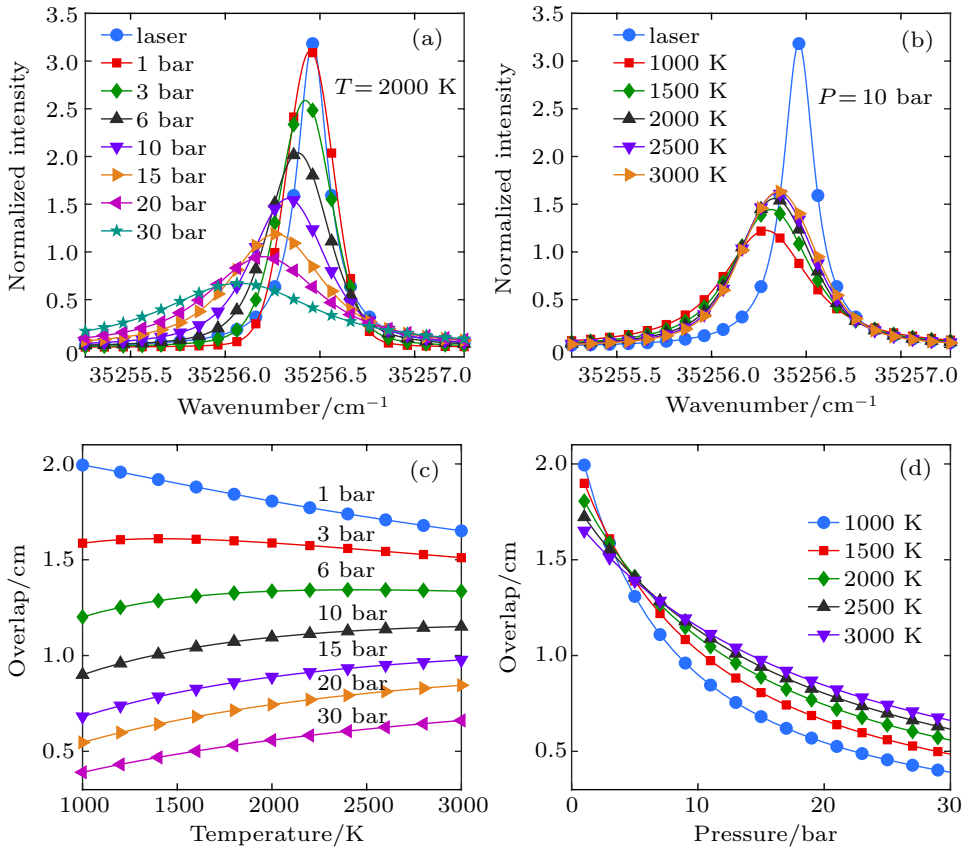


Fig. 2. Typical laser spectrum and absorption spectra of line $Q_1(8)$ of the OH A–X (1,0) band at (a) different pressures and 2000 K, (b) different temperatures and 10 bar. Panels (c) and (d) show the corresponding calculated overlaps assuming the laser frequency is tuned to the center of absorption spectra.

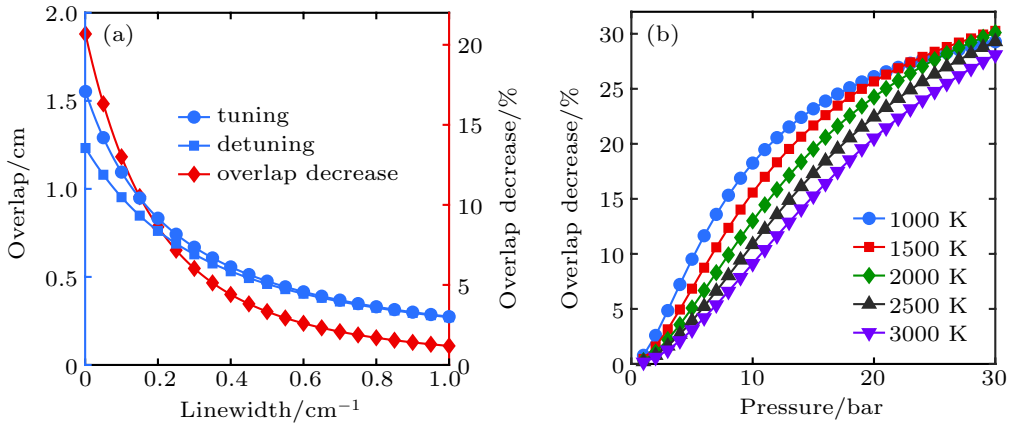


Fig. 3. (a) Calculated overlaps of $Q_1(8)$ for the tuning and detuning cases at 2000 K and 10 bar, with the laser linewidth varying from 0 to 1 cm^{-1}. The detuning-induced overlap decreases are also calculated and shown in the figure. (b) The detuning-induced overlap decreases for different temperatures and pressures, where the laser linewidth is 0.1 cm^{-1}.

3.3. Fluorescence yield

The fluorescence yield represents the fraction of laser-excited molecules that emit fluorescence photons before returning to the ground state. The quantification of the fluorescence yield requires the determination of collisional quenching coefficient. The calculation of collisional quenching, however, is very complicated because it depends on the detailed information of energy transfer. The LASKIN code is employed to simulate the energy transfer in OH-LIF, including collisional quenching, VET, RET, *etc*. A stoichiometric CH_4/air flame is taken as an example to analyse the influence of temperature and pressure on fluorescence yield. The exhaust gases of the flame in chemical equilibrium consist of 71.43% N_2, 0.46% O_2, 18.3% H_2O, 0.36% H_2, 8.53% CO_2, and 0.90% CO, computed by the open-source code Cantera[19] with the GRI-Mech 3.0 chemical mechanism.[20] It should be noted that the gas composition of the flame varies very little in chemical equilibrium for different temperatures and pressures, which can be omitted. The temperature is varied between 1000 K and 2300 K and the pressure is varied from 1 bar to 30 bar. In our case, the OH fluorescence is collected including the overall emission from the A–X (0,0) and (1,1) bands, under excitation of $Q_1(8)$ line in A–X (1, 0) band. The laser pulse is assumed to have the form of $I(t) \propto t^a \exp(-bt)$, with values of $a = 2.5$ and $b = 2 \times 10^8$ s^{-1}, which provides a good approximation of typical laser pulse adopted in OH-LIF measurements.

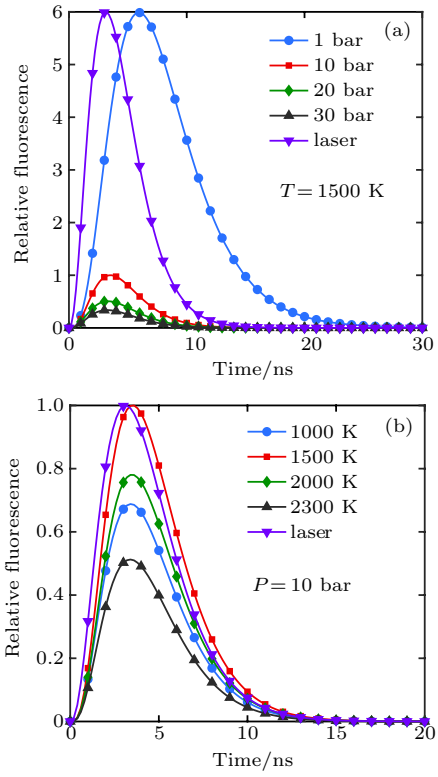


Fig. 4. Temporal profiles of the simulated fluorescence for CH_4/air flame: (a) at different pressures of 1 bar, 10 bar, 20 bar, 30 bar, and constant temperature of 1500 K; (b) at different temperatures of 1000 K, 1500 K, 2000 K, 2300 K, and constant pressure of 10 bar. The laser profile is also shown and marked with solid downward triangles in the figure. The amplitudes of the laser pulse are individually set according to the scales of *y*-axes in each sub-figures.

Figure 4 shows the temporal profiles of the simulated fluorescence for CH_4/air flame. And figure 5 illustrates the relative fluorescence yield as a function of pressure and temperature, respectively. The fluorescence signal lags just behind the laser pulse. As the pressure increases, the fluorescence drops sharply, and its duration reduces, which implies a shorter lifetime of fluorescence. From Fig. 5(a), the fluorescence yield is approximately inversely proportional to pressure at a certain temperature. This is due to the fact that the quenching rate is proportional to the total density population which increases linearly with pressure. As shown in Fig. 4(b), the fluorescence signal varies for different temperatures, but its lifetime remains almost the same. At a certain pressure, the trend of fluorescence yield when increasing temperature has a downward-parabola-like profile, and there appears a peak value at about 1500 K. This is a natural result of the characteristic of RET.[7]

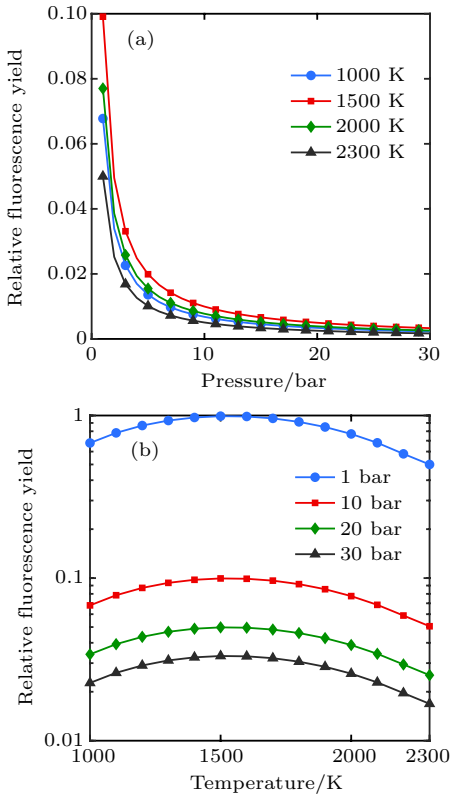


Fig. 5. (a) Relative fluorescence yields as a function of pressure at different temperatures. (b) Relative fluorescence yields as a function of temperature at different pressures. Note the logarithmic scale in sub-figure (b).

It should be pointed out that, the temperature alters the fluorescence yield at an acceptable level, but the high pressure heavily affects the fluorescence yield. The fluorescence yield at 10 bar is only about 1/10 of that at 1 bar and increasing pressure would further decrease the fluorescence yield. Thus it is not easy to detect OH-LIF at high pressure.

4. Experimental validation

The OH-LIF measurements of stoichiometric CH_4/air flame were conducted on McKenna flat burner placed in a

home-made high-pressure chamber, which can operate at a maximum pressure of 15 bar, as reported in Ref. [22]. The pressure of the high-pressure chamber can stabilize at a certain pressure with a deviation less than 1%. The exit velocities were fixed to 5 cm/s in each flame through changing the flow rates of CH_4 and air. The LIF measurement set-up is similar to our previous studies.[23,24] The excitation line for OH was chosen to be $Q_1(8)$ of A–X (1,0), near 283.636 nm. But the exact exciting wavelength was carefully tuning while monitoring the LIF signal, in order to eliminate pressure-dependent frequency-shift effect. The fluorescence was collected with an intensified CCD camera at about 5 mm above the burner surface at pressures from 1 bar to 10 bar with a step of 1 bar. Figure 6 shows the pressure dependence of fluorescence intensity obtained by averaging 50 individual measurements, and the error bars represent the standard derivations. The fluorescence intensity decreases with increasing pressure, which resembles an inverse dependence of pressure. Such behavior is similar to that of fluorescence yield as analyzed in Subsection 3.3. It is experimental validated that the collisional quenching plays a decisive role in fluorescence decrease at high pressure, although the line shape and absorption of OH vary a little at different pressures.

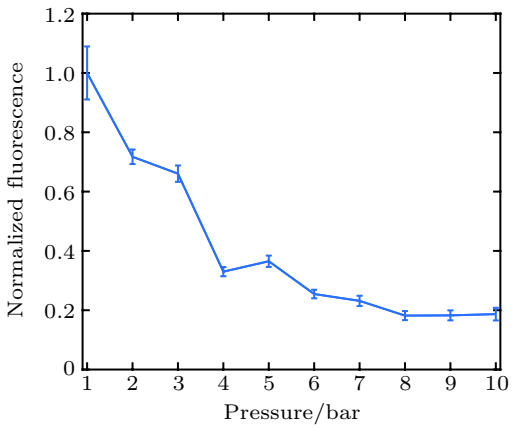


Fig. 6. OH fluorescence signal as a function of pressure for the $Q_1(8)$ of A–X (1,0) at about 5 mm above the burner exit.

5. Conclusion and perspectives

In summary, the effects of temperature and pressure on OH-LIF are numerically studied under the common excitation of A–X (1,0) transition at high pressures. The study firstly analyses the physical processes of LIF in detail. It is found that the fluorescence signal is a complex function of absolute OH concentration, pressure, temperature, and the chemical composition of flame. Operations at high pressures require a careful choice of excitation line. Through the calculation of Boltzmann fraction, the $Q_1(8)$ line in A–X (1,0) band of OH presents the minimum temperature dependence, and is perfect for OH-LIF. At high pressures, LIF measurements suffer from the collision-induced effects, such as absorption lineshape broadening, central-frequency shifting and collisional quenching. The absorption spectra of OH are calculated using HITRAN database with a modified HAPI-based Python function. The overlap integral gets lower due to the absorption lineshape broadening as pressure increases, which leads to smaller excitation efficiency. It is of great importance to take into account central-frequency shifting that cannot be omitted at high pressures. And the laser frequency should be tuned to the center of the absorption spectrum according to the predetermined or estimated pressure. The fluorescence yield is estimated based on the LASKIN calculation, taking into considering collisional quenching, VET, RET in the upper states. It is illustrated the fluorescence yield is approximately inversely proportional to pressure at a certain temperature. And the temperature would alter the fluorescence yield, but at an acceptable level. The OH-LIF measurements of flat CH_4/air in high-pressures chamber validate the decisive contribution of collisional quenching on fluorescence decrease at high pressure. To summarize, it is important to keep in mind that, the temperature dependence of fluorescence is dominated by the Boltzmann fraction, and the pressure dependence is primarily governed via the overlap integral and fluorescence yield. And the collisional quenching plays a decisive role in fluorescence decrease at high pressure. These results illustrate the physical processes of OH-LIF, and would provide useful suggestions for high-pressure application of OH-LIF.

Acknowledgment

The authors would like to thank the LASKIN group for providing the software.

References

[1] Yang Z, Peng J, Yu X, Sun S, Meng S and Xu H 2016 *Spectrosc. Lett.* **49** 482
[2] Kohse-Höinghaus K 1994 *Prog. Energy Combust. Sci.* **20** 203
[3] Boxx I, Slabaugh C, Kutne P, Lucht R P and Meier W 2015 *Proc. Combust. Inst.* **35** 3793
[4] Zhou B, Brackmann C, Li Z, Aldén M and Bai X 2015 *Proc. Combust. Inst.* **35** 1409
[5] Lv L, Tan J and Zhu J 2017 *Acta Astronaut.* **139** 258
[6] Chan C and Daily J W 1980 *Appl. Opt.* **19** 1357
[7] Chen S, Su T, Zheng Y, Chen L, Liu T, Li R and Yang F 2016 *Chin. Phys. B* **25** 060703
[8] Matynia A, Idir M, Molet J, Roche C, de Persis S and Pillier L 2012 *Appl. Phys. B* **108** 393
[9] Singla G, Scouflaire P, Rolon C and Candel S 2006 *Combust. Flame* **144** 151
[10] Rahmann U, Bulter A, Lenhard U, Dusing R, Markus D, Brockhinke A and Kohse-Höinghaus K *LASKIN — A Simulation Program for Time-Resolved LIF-Spectra*, University of Bielefeld, Faculty of Chemistry, Physical Chemistry I, http://pc1.uni-bielefeld.de/∼laskin
[11] Li Y and Gupta R 2003 *Appl. Opt.* **42** 2226

[12] Luque J and Crosley D R 1998 *J. Chem. Phys.* **109** 439
[13] Singla G, Scouflaire P, Rolon J C and Candel S 2007 *J. Propul. Power* **23** 593
[14] Gordon I E, Rothman L S, Hill C, Kochanov R V *et al*. 2017 *J. Quantum Spectrosc. Radiat. Transfer* **203** 3
[15] Goldman A, Schoenfeld W G, Goorvitch D, Chackerian C, Dothe H, Mélen F, Abrams M C and Selby J E A 1998 *J. Quantum Spectrosc. Radiat. Transfer* **59** 453
[16] Davidson D F, Roehrig M, Petersen E L, Di Rosa M D and Hanson R K 1996 *J. Quantum Spectrosc. Radiat. Transfer* **55** 755
[17] Kochanov R V, Gordon I E, Rothman L S, Wcisło P, Hill C and Wilzewski J S 2016 *J. Quantum Spectrosc. Radiat. Transfer* **177** 15
[18] Luque J and Crosley D R *LIFBASE: Database and spectral simulation* (version 1.5), SRI International Report MP 99-0091999
[19] Goodwin D G, Speth R L, Moffat H K, Weber B W 2018 *Cantera: An object-oriented software toolkit for chemical kinetics, thermodynamics and transport processes* Version 2.4.0.
[20] Smith G P, Golden D M, Frenklach M, Moriarty N W, Eiteneer B, Goldenberg M, Bowman C T, Hanson R K, Song S, Gardiner W C, Jr V V L, Qin Z *GRI-Mech 3.0*. http://www.me.berkeley.edu/gri_mech/
[21] Kienle R, Lee M P and KohseH Inghaus K 1996 *Appl. Phys. B* **62** 583
[22] Yan B, Chen L, Li M, Chen S, Gong C, Yang F, Wu Y, Zhou J and Mu J 2020 *Chin. Phys. B* **29** 024701
[23] Tu X, Liu B, Wang L, Qi X, Yan B, Mu J, Chen S and Qin F 2019 *Proc. SPIE* **11046** 110462K
[24] Chen S, Su T, Li Z, Bai H, Yan B and Yang F 2016 *Chin. Phys. B* **25** 100701